

Numerical study on steady-state cracking of composites

Enhua Yang ^{*}, Victor C. Li

Civil and Environmental Engineering, University of Michigan, MI 48109, USA

Received 12 June 2006; accepted 12 July 2006

Available online 18 September 2006

Abstract

This article presents a numerical study on the steady-state cracking in brittle matrix composites. While steady-state cracking underlies the phenomenon of multiple cracking, an important mechanism to achieve tensile ductility in such materials, it is difficult to capture experimentally. This paper provides a numerical approach to simulate steady-state cracking behavior in reinforced brittle matrix composites. From computational results, the previously derived analytic condition of steady-state cracking is confirmed and steady-state crack propagation can be digitally visualized.

© 2006 Elsevier Ltd. All rights reserved.

Keywords: B. Modelling; B. Matrix cracking; C. Damage mechanics; A. Short-fibre composites; C. Finite element analysis (FEA)

1. Introduction

In some composite systems when the applied ambient stress exceeds the matrix cracking strength, a flat crack can form after initiating from a defect site and extends infinitely through the matrix. In this scenario, the crack opening δ and the ambient loading σ_∞ remain constant and bridging ligaments sustain and pass the load without rupturing and diminishing. This behavior is known as steady-state cracking. Further loading causes crack initiation from another defect site and subsequent flat crack propagation occurs. Repeated formation of such steady-state cracks results in multiple cracking and strain-hardening of the composite. This deformation mechanism has been observed experimentally in several reinforced brittle matrix composites [1–3] and is important for the converting brittle materials into ductile materials in tension.

Steady-state cracking in the present study is defined as crack extension under constant ambient load independent of crack length. Specifically, the crack propagates at constant crack width, i.e. in a flat crack mode, Fig. 1(a), with

crack flanks bridged by fibers. Under this circumstance, the crack tip advances without knowing any difference in its surrounding environment, including the loading, crack shape, stress and strain fields, and boundary conditions. Conversely, extension of a Griffith type crack, Fig. 1(b), is accompanied by a continuous drop in ambient load and a widening in crack opening. (We define here a “Griffith type crack” as essentially a Griffith crack which has part of the crack opening profile near the crack tip region modified by the presence of cohesive traction due to matrix retention and/or fiber bridging, but otherwise the same as a standard Griffith crack.) Although steady-state cracking theory has been established for many years, it has not yet been observed experimentally due to test difficulties. In this study, a numerical approach will be employed to simulate steady-state crack propagation and to verify the validity of the steady-state cracking theory.

In the following sections, the theoretical background of steady-state cracking is introduced, and the cohesive traction model which was employed in this study to calculate the cracking behavior is shown in Section 3. Sections 4 and 5 display the results and discussion for the Griffith type and the steady-state crack propagation, respectively. Section 6 gives the conclusion.

^{*} Corresponding author. Tel.: +1 734 763 1315; fax: +1 734 764 4292.
E-mail address: ehy@umich.edu (E. Yang).

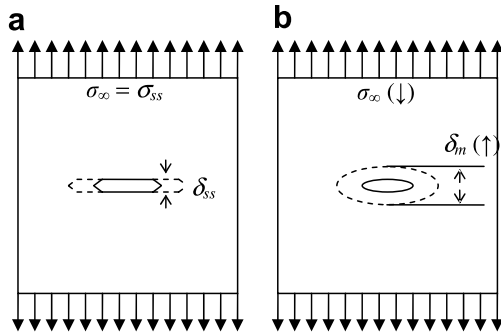


Fig. 1. (a) Steady-state cracking with constant ambient load σ_{ss} and constant crack opening δ_{ss} (flat crack); and (b) Griffith crack (an oval shape crack) with a descending ambient load and a widened crack opening.

2. Condition for steady-state cracking

The theoretical foundation of multiple cracking was first studied by Aveston et al. [4] who analyzed this phenomenon for an aligned continuous fiber reinforced brittle matrix composite. Later, Marshall and Cox [5] employed the J-integral method to calculate steady-state cracking stress σ_{ss} and proposed a more general solution for the condition of steady-state cracking:

$$\sigma_{ss} \delta_{ss} - \int_0^{\delta_{ss}} \sigma(\delta) d\delta = J_{tip} \tag{1}$$

where J_{tip} is the crack tip toughness and $\sigma(\delta)$ is the spring law of the material elements bridging the crack surfaces (Fig. 2). Eq. (1) can also be derived based on the energy balance concept and expresses the energy exchange per unit crack advance during steady-state cracking. The left hand side of Eq. (1) may be interpreted as the net energy input by external work (first term) less the energy consumed by the bridging elements which open from 0 to δ_{ss} (second term), and represents the complementary energy of the $\sigma(\delta)$ curve (shaded area in Fig. 2). Hence, Eq. (1) dictates that the net energy available for driving the crack must be equal to the crack tip toughness during steady-state crack extension. This is an alternative definition of steady-state cracking in the present context. That is, the net energy available to drive the crack tip propagation is invariant with the crack length.

Recognizing that the left hand side of Eq. (1) reaches a maximum, J'_b , steady-state cracking is guaranteed when

$$J'_b \equiv \sigma_0 \delta_0 - \int_0^{\delta_0} \sigma(\delta) d\delta \geq J_{tip} \tag{2}$$

where J'_b is the maximum complementary energy defined as the hatched area in Fig. 2.

Eq. (2) has been recognized as an important criterion in designing reinforced brittle matrix composites. Li et al. utilized this criterion in conjunction with a $\sigma(\delta)$ formulated for short randomly distributed fibers [6] in the successful development of engineered cementitious composite (ECC) with 5% tensile strain capacity [7].

3. Cohesive traction model with two interface types

To simulate the behavior of crack extension, the cohesive traction model provides an effective approach and relatively precise solution [8]. In this study, the cohesive traction model was realized by employing interface element with the user-defined cohesive traction law in the crack plane. The simulations were performed using a commercial finite element analysis (FEA) software DIANA. The interface element with the user-defined cohesive traction law is a standard element formulation in DIANA.

Fig. 3 gives the details of the model. A two dimensional plate with 160 mm in width and 100.5 mm in length is modeled using the finite element method. Due to x- and y-axis symmetries, only a quarter of the plate is modeled. The boundary conditions are fixed in the y direction for the bottom line and fixed in the x direction for the left sideline. The plate is subject to an ambient uniaxial tensile load σ_{∞} . The matrix element is assumed to act linear-elastically. Interface elements are used to simulate the developing crack and are assigned the user-defined cohesive traction law as material property. Except for those elements representing a pre-existing crack, they are assumed to be linear elastic until a predefined tensile strength f_t is reached. After that, the cohesive behavior follows the imposed cohesive traction law. Specifically, two sets of interface elements are deliberately employed as shown in Fig. 3. Interface 1 and 2 can be assigned different operative traction behavior for different investigation purposes. For example, a zero bridging in interface 1 and a matrix retention law in interface 2 represents a traction-free center through-crack in a two dimensional plate. Matrix retention is used to represent the break-down tension-softening behavior of the matrix (see Fig. 4). As another example, interface 1 and 2 can be assigned a bridging law and a total cohesive traction curve, respectively. In this scenario, interface 1 represents a cracked interface but still with cohesive traction associated with bridging only (e.g. fiber) and interface 2 is an (as yet) uncracked interface with assigned cohesive traction combining both

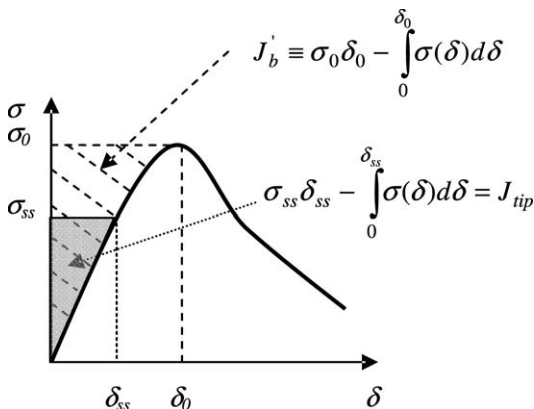


Fig. 2. A bridging law which satisfies steady-state cracking condition.

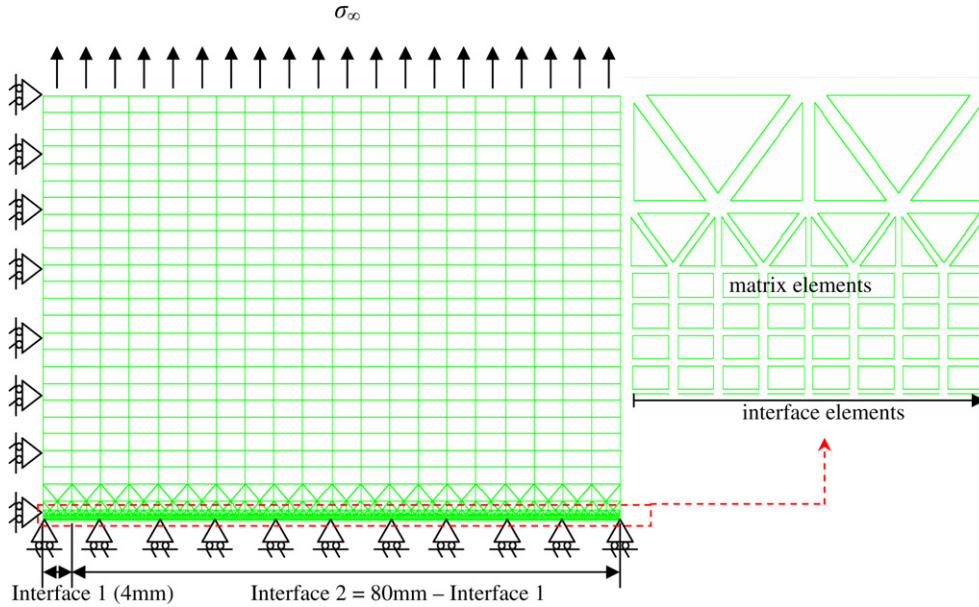


Fig. 3. Cohesive traction model with two interface types.

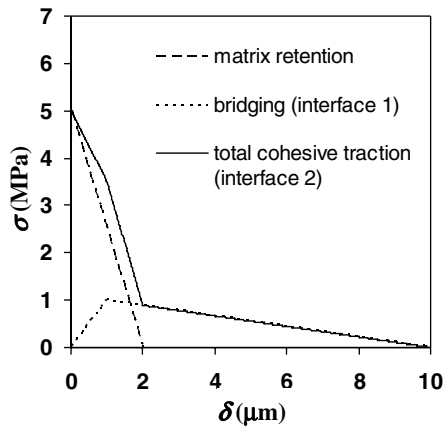


Fig. 4. Bridging curve and matrix retention with $J'_b < J_{tip}$.

matrix retention and fiber bridging action. Interface 2 effectively becomes part of interface 1 when matrix retention is exhausted as the crack opening increases. The philosophy behind this approach reflects the recognition that the matrix breakdown and the bridging (e.g. fiber) are two separate and distinct physical processes. This is consistent with the bridged crack concept first suggested by Marshall and Cox [5].

In the following sections, several scenarios (i.e. Griffith type cracking and steady-state crack propagation) were examined by incorporating this cohesive traction model.

4. Simulation of Griffith type cracking

Base on the theory embodied in Eq. (2), if the condition of steady-state cracking is not satisfied, a Griffith type crack, with enlarging crack opening δ as a function of crack length, should result. For the Griffith type crack,

the near tip crack opening profile is not described by the typically elliptical shape as in the case of the classical Griffith crack, due to cohesive traction which reduces the opening. Fig. 4 shows a bridging law and a matrix retention law in which J'_b (0.5 J/m^2) is less than J_{tip} (5 J/m^2), so that Eq. (2) is violated. The value of J_{tip} can be calculated from the area under the matrix retention curve. The value of J'_b is the area to the left of the bridging law up to the peak bridging stress.

Fig. 5 shows the computational results when the above cohesive tractions are assigned to interface 1 and 2. The computation was conducted by load control and an arch-length method [9] was used as the solution method. The arch-length method which is automatically implemented in DIANA has the advantage of solving problems with high nonlinearity which is likely to be the case in the present study. As can be seen in Fig. 5(a), after the peak load, a descending ambient stress σ_∞ is accompanied by a continuously increasing mid-crack opening δ_m (measured at the center of the crack). Fig. 5(b) plots a quarter of the crack opening profile after the peak load. By symmetry, an enlarging oval shape crack forms with a descending σ_∞ . The concave shape near the crack tip region (circular part in Fig. 5(c)) is a result of matrix retention and bridging traction. Fig. 5(c) shows δ_m versus crack length (L , measured in terms of the length of interface with $\delta > 0$) curve. By plotting $\Delta\delta_m/\Delta L$ (secant slope calculated from two adjacent data points) versus L curve as shown in Fig 5(d), it is found that the change in mid-crack opening per unit crack advance $\Delta\delta_m/\Delta L$ approaches a constant (0.09) which implies a continuously widening crack as the crack tip extends. Continuously enlarging in crack opening causes the exhausting of bridging, and therefore it has to be a Griffith type crack.

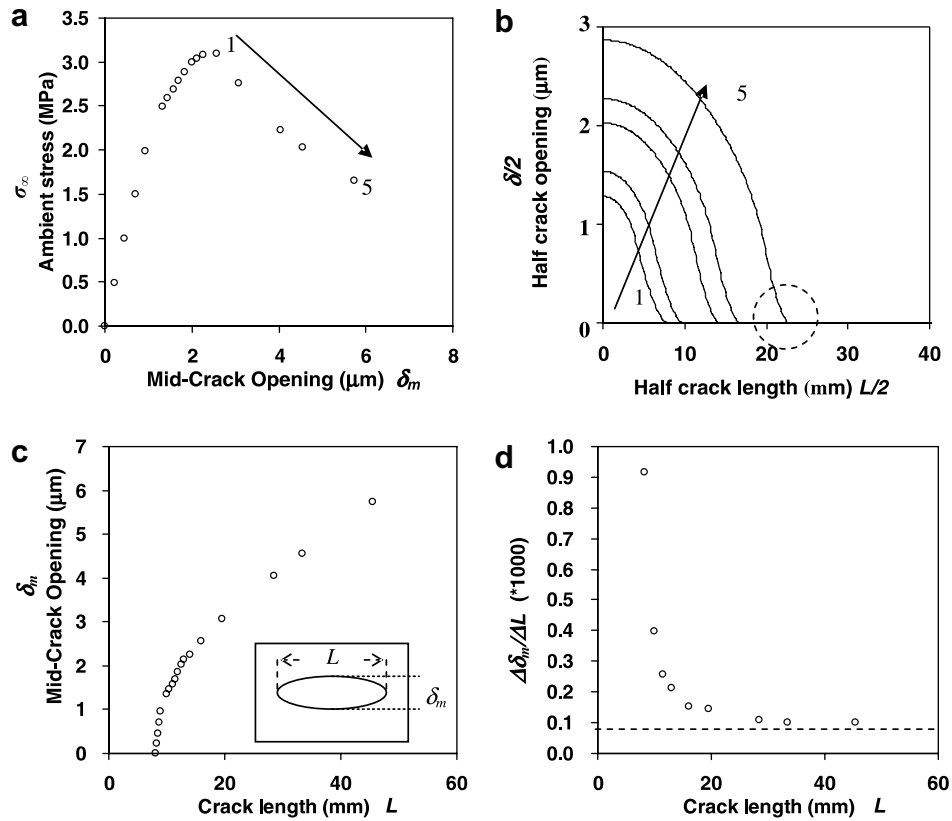


Fig. 5. Computational results of Griffith type cracking where cohesive tractions in Fig. 4 are applied to interface 1 and 2, respectively.

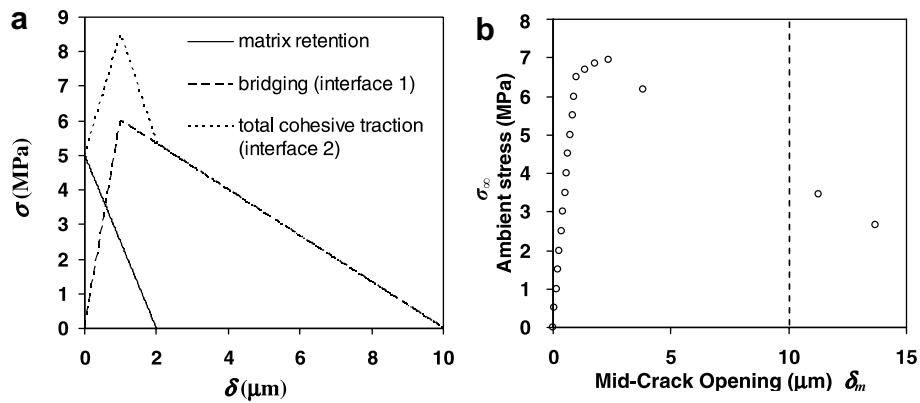


Fig. 6. (a) Bridging law with substantial bridging strength; and (b) computational result of $\sigma_\infty - \delta_m$.

It may be argued that the Griffith type cracking behavior described above is a result of low bridging strength ($\sigma_0 = 1$ MPa) compared to the matrix strength ($f_t = 5$ MPa). However, another computation attempt shows that even when the bridging strength ($\sigma_0 = 6$ MPa) is larger than the matrix strength ($f_t = 5$ MPa) as shown in Fig. 6(a), crack propagation remains in a Griffith type mode. For this case, J'_b (3 J/m^2) is set to remain lower than J_{tip} (5 J/m^2) so that the steady-state criterion (Eq. (2)) is still violated. Fig. 6(b) plots the computed ambient load versus the mid-crack opening curve. Again, a continuously increasing crack opening is observed beyond the peak load. At a cer-

tain point, the crack opening exceeds $10 \mu\text{m}$, which indicates the exhausting of the fiber bridging capacity (Fig. 6(a)) and a traction free Griffith type crack results.

From the above analyses, it is concluded that no matter how strong the fiber bridging is, a Griffith type crack will form as long as Eq. (2) is violated, that is, when the complementary energy J'_b is smaller than the matrix toughness J_{tip} . In ductilizing brittle matrix composites, this result reveals an important information that a composite with strong bridging is not necessary a tough material. This concept; however, has not been widely accepted by researchers.

5. Simulation of steady-state cracking

To demonstrate steady-state cracking, a bridging curve with larger J'_b is assigned to interface 1. Fig. 7 shows the matrix retention and bridging laws employed for this study. In this case, J'_b is 12 J/m^2 which is larger than J_{tip} (5 J/m^2) so that Eq. (2) is satisfied.

It has to be pointed out that direct calculation and simulation of steady-state cracking is difficult. Mathematically speaking, steady-state cracking represents infinite

solutions in terms of crack length for a given load. In other words, infinite equilibrium states of different crack length can be found at the steady-state cracking stress (σ_{ss}). However, it is impossible for a FEA program to find more than one solution/equilibrium state. An alternate way to simulate steady-state cracking is to calculate the cracking strength of the plate for different crack lengths, specifically, different length of interface 1 on which only fiber bridging (no matrix retention) is imposed. A constant ambient load for different imposed crack lengths, if found, implies steady-state cracking. This concept is somewhat analogous to the displacement control method utilized in many FEA.

Fig. 8 shows the computational results of the plate with different length of interface 1 ranging from 4 mm to 44 mm. As can be seen in Fig. 8(a), a stable crack growth is found before the peak load. After that, a descending ambient stress accompanied by an increase in crack length indicates unstable cracking. However, this unstable crack propagation is bounded and the ambient stress approaches a constant value (σ_{ss}) with further crack extension. Fig. 8(b) displays a quarter of the crack opening profile after the peak load. Interestingly, the crack starts with an oval shape and tends to propagate in a flat manner after a certain length of propagation. Fig. 8(c) and (d) show the $\delta_m - L$ and the $\Delta\delta_m/\Delta L - L$ curves, respectively. It can be seen

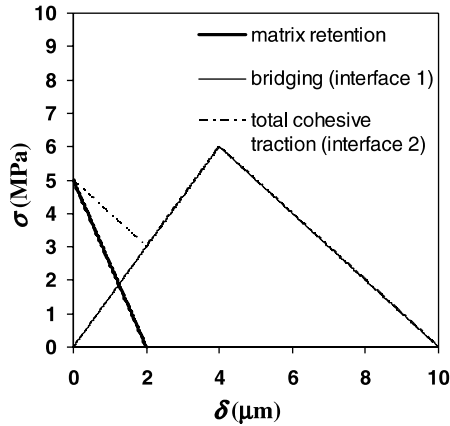


Fig. 7. Bridging law with $J'_b > J_{tip}$.

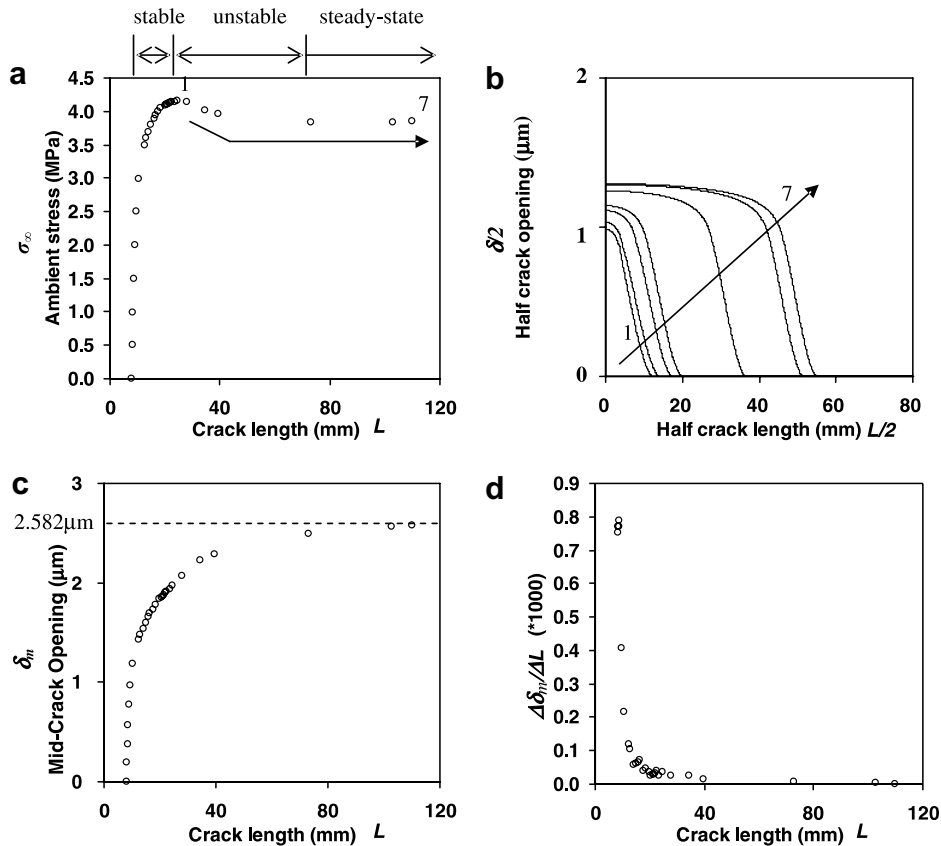


Fig. 8. Computational results of steady-state cracking. Stage numbers represent the ambient stress states in (a) and the corresponding crack profiles are shown in (b). Mid-crack opening behavior is shown in (c) and (d).

that the crack opening approaches a constant (δ_{ss}) when the crack tip moves forward and $\Delta\delta_m/\Delta L$ approaches zero which suggests the cessation of crack widening as it extends in length. These observations confirm the attainment of steady-state cracking.

According to the condition of steady-state cracking (Eq. (1)), the complementary energy J'_b should equal the matrix toughness J_{tip} at steady-state. From the computational results shown above, the crack opening at steady-state δ_{ss} in this case is 2.582 μm (Fig. 8(c)). Using this information combined with the given bridging law $\sigma(\delta)$, the complementary energy J'_b at steady-state can be calculated and the value is 4.9992 J/m^2 , which is very close to the theoretical value ($J'_b = J_{tip} = 5 \text{ J}/\text{m}^2$). Through this check, the condition for steady-state cracking is further confirmed.

From the above discussions, it is clear that appropriate bridging traction relations, in contrast to strong bridging, are required in order to achieve steady-state cracking and to ductilize brittle matrix composite. This fact has been recognized and implemented in designing a short fiber reinforced brittle matrix composites – Engineering Cementitious Composites (ECC) (Li et al., 2001). In ECC, the complementary energy (J'_b) was maximized through tailoring proper fiber/matrix interface properties. On the other hand, J_{tip} can be minimized through matrix modification. However, excessively weak matrix (lower J_{tip}) usually introduces low compressive strength which is not desirable for most building materials. Eq. (2) allows a systematic means of searching for optimal combinations of matrix toughness (J_{tip}) and fiber bridging properties (J'_b).

6. Conclusion

The research demonstrates and simulates steady-state cracking in composites utilizing a numerical approach.

The numerical results establish without a doubt that the steady-state cracking criterion is a fundamental principle that must be satisfied for ductilizing brittle matrix composites via multiple cracking. As also demonstrated from experimental research (Li et al., 2001), deliberate control of the bridging law through tailoring of the composite constituents, as governed by the steady-state cracking criterion, is key to attaining ductile composites.

The cohesive traction model with two interface types provides good results in simulating single crack propagation for a broad range of composite materials. This model will be extended to simulate the multiple-cracking behavior in reinforced brittle matrix composites in the future.

References

- [1] Marshall DB, Evans AG. Failure mechanisms in ceramic–fiber/ceramic–matrix composites. *J Am Ceram Soc* 1985;68:225–31.
- [2] Phillips DC. The fracture energy of carbon-fiber reinforced glass. *J Mater Sci* 1972;7:1175–91.
- [3] Majumdar AJ. Glass fiber reinforced cement and gypsum products. *Proc R Soc* 1970;A319:69.
- [4] Aveston J, Cooper GA, Kelly A. Single and multiple fracture. *Prop Fiber Compos* 1971:15–26.
- [5] Marshall DB, Cox BN. A J-integral method for calculating steady-state matrix cracking stresses in composites. *Mech Mater* 1988;7:127–33.
- [6] Lin Z, Kanda T, Li VC. On interface property characterization and performance of fiber reinforced cementitious composites. *J Conc Sci Eng* 1999;1:173–84.
- [7] Li VC, Wang S, Wu C. Tensile strain-hardening behavior of PVA-ECC. *ACI Mater J* 2001;98:483–92.
- [8] Hillerborg A, Modeer M, Petersson PE. Analysis of crack formation and crack growth in concrete by means of fracture mechanics and finite elements. *Cement Conc Res* 1976;6:773–82.
- [9] Cook RD, Malkus DS, Plesha ME, Witt RJ. Concepts and applications of finite element analysis. Wiley Publication; 2002 [chapter 17].